THE JOURNAL OF PHYSICAL CHEMISTRY Letters

Letter

pubs.acs.org/JPCL

Cubic Perovskite Structure of Black Formamidinium Lead Iodide, α-$[HC(NH_2)_2]PbI_3$, at 298 K

Mark T. Weller,* Oliver J. Weber, Jarvist M. Frost, and Aron Walsh

Centre for Sustainable Chemical Technologies and Department of Chemistry, University of Bath, Bath, BA2 7AY, United Kingdom

Supporting Information

ABSTRACT: The structure of black formamidinium lead halide, α-$[HC(NH_2)_2]PbI_3$, at 298 K has been refined from high resolution neutron powder diffraction data and found to adopt a cubic perovskite unit cell, a = 6.3620(8) Å. The trigonal planar $[HC(NH_2)_2]^+$ cations lie in the central mirror plane of the unit cell with the formamidinium cations disordered over 12 possible sites arranged so that the C−H bond is directed into a cube face, whereas the $-NH_2$ groups hydrogen bond (NH···I = 2.75−3.00 Å) with the iodide atoms of the $[PbI_3]^-$ framework. High atomic displacement parameters for the formamidinium cation are consistent with rapid molecular rotations at room temperature as evidenced in *ab initio* molecular dynamic simulations.

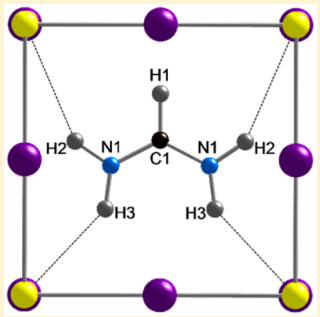

Hybrid halide perovskite solar cells have captured significant research attention due to the demonstration of their use in highly efficient photovoltaic devices produced via low-cost deposition methods.[1−7] The complete structure and dynamics of the systems, covering the inorganic framework, the molecular cation and their mutual interactions, all impact upon the photovoltaic performance of these materials; understanding these fundamental structural and motional behaviors are central to developing this class of materials toward devices.[8,9] The bulk of research has focused on methylammonium lead iodide (MAPI); however, the formamidinium cation $HC(NH_2)_2^+$ (FA) also templates a lead iodide perovskite-type structure for $HC(NH_2)_2PbI_3$ (FAPI) with fully vertex connected PbI_6 octahedra. Solar cells based on FAPI with a maximum power conversion efficiency of 20.1% have been recently demonstrated.[10] The increase of effective cation radius on switching from the methylammonium to the formamidinium cation decreases the optical band gap from 1.54 to 1.47 eV, extending absorption into the near-infrared.[11]

The synthesis, structure, and phase behavior of $FAPbI_3$ has been reported by Stoumpos et al.[12] FAPI crystallizes at room temperature as a nonperovskite, hexagonal yellow phase (δ-phase), in the space group $P6_3mc$, and formed from face-sharing PbI_6 octahedra linked into chains. The structure of the black perovskite phase of FAPI (α-phase), which is formed at higher temperatures, was refined in this work from single crystal X-ray diffraction data using trigonal space groups and 3-fold disordered FA cation. $FASnI_3$ has been reported as adopting a cubic perovskite structure.[13]

The low stability of hybrid perovskite materials toward heat and moisture has been discussed widely and results from the facile phase transitions at or near room temperature and formation of hydrated phases. These stability issues have hindered attempts to scale technology using these materials and serious question marks remain over stability even for sealed devices.[14] The formamidinium cation is believed to exhibit even lower stability than methylammonium.[12] $MAPbI_3$ and $MA_xFA_{1-x}PbI_3$ have recently been shown to be efficient halide ion conductors[15] and undergo structural changes under polarization[16] or illumination.[17] Solid solutions, for example, $FAPI/MAPbBr_3$ have been employed in high efficiency perovskite cells, reportedly displaying greater stability than the parent compounds.[15,18,19] Binek et al.[20] have studied the stabilization of thin films of α-FAPI by inclusion of up to 15% MA^+.

We have previously demonstrated the power of neutron powder diffraction in determining the atomic structure in hybrid perovskite compounds as it circumvents many of the factors limiting the usefulness of single crystal X-ray diffraction for analysis of these hybrid systems. As well the identification of light atom positions, including hydrogen, and distinguishing carbon from nitrogen, it also avoids difficulties in structure refinement stemming from multiple twinning or domain structure of crystals.[9]

Neutron powder diffraction data were obtained on the HRPD instrument at ISIS as summarized in the Supporting Information. Initial inspection of the data showed far fewer reflections than predicted by the hexagonal unit cell model for FAPI proposed by Stoumpos (see Supporting Information Figures S1 and S2) indicating that the true unit cell was probably simpler than used in that work. Peak positions were extracted for 20 reflections and indexed manually from their d-spacings to give a cubic unit cell of dimension ∼6.36 Å. This cell indexed all the reflections observed except for a few minor features associated with diffraction from the vanadium slab can

Received: July 7, 2015
Accepted: August 4, 2015
Published: August 4, 2015

DOI: 10.1021/acs.jpclett.5b01432
J. Phys. Chem. Lett. 2015, 6, 3209−3212

(at, for example, 2.14 Å) and off-center aluminum cryoloop tail (these were readily identified from their *d*-spacings and varying intensities and positions in the different HRPD data banks). This cubic unit cell is similar to that found for the cubic phase adopted by MAPI above 327 K though it is slightly larger, which is indicative of the larger size of the formamidinium cation compared to methylammonium. In order to check the validity of this new choice of unit cell, powder X-ray diffraction (PXD) data were also collected from a FAPI phase, Supporting Information Figure S3, and could also be fully indexed of a simple cubic unit cell of dimensions 6.36 Å. Note that the sensitivity of neutron diffraction data to light elements, such as C, N, and H, shows that these atom positions can also be defined using the simple cubic description—and any deviations from cubic to hexagonal symmetry would direct diffraction intensity into additional reflections. Le Bail fits to the PXD data were undertaken using both the new cubic unit cell and the original hexagonal unit cell and showed an excellent fit (χ^2 = 2.18) using the simple cubic cell, Supporting Information, Figure S4.

A structure model for cubic FAPI was developed using that of cubic MAPI with the lead iodide framework described using nontilted PbI_6 octahedra in the space group *Pm*-3*m*. The position of a planar formamidinium cation within this cubic framework was energy minimized within density functional theory (DFT, PBEsol functional) within the regular 6.36 Å cube and found to adopt an orientation with the N−CH−N molecular ion fragment lying in the unit cell midplane, the (200) plane, with the C−H bond pointing directly toward the cube face (thereby minimizing CH···I interactions), and the C−N bonds directed toward adjacent cube faces. This allows the $-NH_2$ groups to be orientated toward the unit cell edges with the potential formation of NH···I hydrogen bonds. Overall, this produces 12 possible orientations for the triangular-planar formamidinium cation in the cubic cage: six orientations of the C−H bond, identified in this work as the *y* direction, and two orientations for the N−C−N plane, in *xy* and *yz*. Reorientation of the organic cation around these 12 orientations would be expected and has been studied by molecular dynamics, vide infra. The crystallographic description of this model in the space group *Pm*-3*m* is very simple with all the atoms on a single mirror plane; the carbon, C, and the directly bonded hydrogen, H1, both located on the 6-fold (1/2, *y*, 1/2), 6f site, with $y \sim 0.55$ and 0.64 for C and H1, respectively, both with site occupancy 0.1667 representing the six possible formamidinium orientations. A single nitrogen position, (*x*, *y*, 1/2), 24l, with occupancy 0.0833, and two amine hydrogen positions also in the molecular plane on 24l, H2 near (0.81, 0.54, 0.5) and H3 near (0.70, 0.29, 1/2), site occupancies 0.0833. Thus, only 5 atom positions and 8 refinable coordinates are required to define the 12 different orientations of the complete planar $[H_2N{-}CH{-}NH_2]^+$ cation. Pb was placed on 1a (0,0,0) and I on 3d (1/2, 0,0) and the refinable coordinates for the C, N, and H atoms were initially set at values derived from the energy minimization. Isotropic atomic displacement parameters (ADPs) for all atoms were set initially at 0.05 Å^2. This model immediately produced a good overall fit to the data and refinement of profile parameters, unit cell parameter, background functions etcetera, led to a χ^2 value of only ∼4. Refinement of lead and iodine ADPs, anisotropic for iodine, reduced χ^2 to 3.5 and showed thermal motion for the iodine atom to be strongly perpendicular to the Pb−I−Pb direction as found previously in MAPI due to octahedral tilting. ADPs were constrained to a single value for all formamidinium atom sites and this value was refined to yield a value of approximately 0.14 Å^2 with χ^2 = 3.05 indicating significant thermal motion and reorientation of this structural element. Final stages of the refinement included an investigation of the formamidinium cation position which was permitted to translate as a rigid body in the *y* direction; a translation of the whole molecule, with the C−H bond moving toward the cube face by approximately 0.25 Å, yielded the final structural model given in Table 1 and χ^2 = 2.62. Final profile fits to the neutron powder diffraction data are given in Figure 1.

Table 1. Final Refined Atomic Positions

atom	*x*[d]	*y*	*z*	$U_{iso}/U_{eq} \times 100$/Å^2
C1	0.5	0.5726(3)[c]	0.5	12.29(23)
N1	0.6820	0.4781(3)[c]	0.5	= C1 U_{iso}
H1	0.5000	0.7447(3)[c]	0.5	= C1 U_{iso}
H2	0.8142	0.5680(3)[c]	0.5	= C1 U_{iso}
H3	0.7025	0.3179(3)[c]	0.5	= C1 U_{iso}
Pb1	0.0	0.0	0.0	2.95(7)
I1	0.5	0.0	0.0	8.20[b]

[a]Space group *Pm*3*m*, *a* = 6.3620(8) Å, *V*= 257.51(5) Å^3. R_{wp}(all) = 1.53%, R_{wp}(all) = 1.20%, R_{wp}(−background) = 4.79%, R_p(−background) = 3.04%, 114 reflections [b]U_{eq} U_{11} = 2.09(20) Å^2 U_{22} = U_{33} = 11.25(17) Å^2 [c]Constrained to have equal shift from DFT modeling values [d]Values from DFT modeling, not refined

The structure of black FAPI, $[H_2N{-}CH{-}NH_2][PbI_3]$ at room temperature consists of a cubic lead iodide, $[PbI_3]^-$ perovskitic framework surrounding orientationally disordered, planar $[H_2N{-}CH{-}NH_2]^+$ cations, Figure 2. The FAPI lattice parameter, 6.3620(8) Å, and cell volume, 257.51(5) Å^3, are significantly larger than those of MAPI (at 298 K), the reduced lattice parameter is 6.304 Å and cell volume 250.5 Å^3, reflecting the larger organic cation size. The Pb−I bond lengths are increased to 3.181(4) Å, implying the lead iodide framework is under some expansive stress with weak Pb−I bonds. This stress may be the origin of the facile phase transition to the yellow phase of FAPI where the Pb−I bonds are significantly shorter. Also of interest are the extracted ADPs for the iodine atom site which show the expected strong anisotropic motion perpendicular to the Pb−I−Pb direction, similar values to those found for iodine in MAPI and representing a soft lead iodide framework.

The refined position of the FA^+ cation within the cubic cage is close to that predicted from the equilibrium athermal structure obtained from DFT-PBEsol calculations. Such calculations tend to underestimate the importance of weak hydrogen bonds such as the NH···I interactions found in FAPI and the cation adopts a site, which allows both terminal amine hydrogen atoms to form weak NH−I hydrogen bonds with the inorganic framework N(H2)···I at 2.992 Å and N(H3)···I at 2.770 Å. This position also maintains the C−H1 to iodide distances at, nonbonded, 3.572 Å. Information on the temporal behavior of the cation positions was obtained from molecular dynamics simulations at 300 K (on the DFT-PBEsol energy landscape; 200 ps production runs using a time-step of 0.5 fs). The molecule is rotationally active around room temperature with a preference for alignment of the C−H bond along ⟨100⟩, in agreement with the structure refinement from powder neutron diffraction, with a time constant of ∼2 ps associated with the rollover process. A video of the rotational dynamics

DOI: 10.1021/acs.jpclett.5b01432
J. Phys. Chem. Lett. 2015, 6, 3209−3212

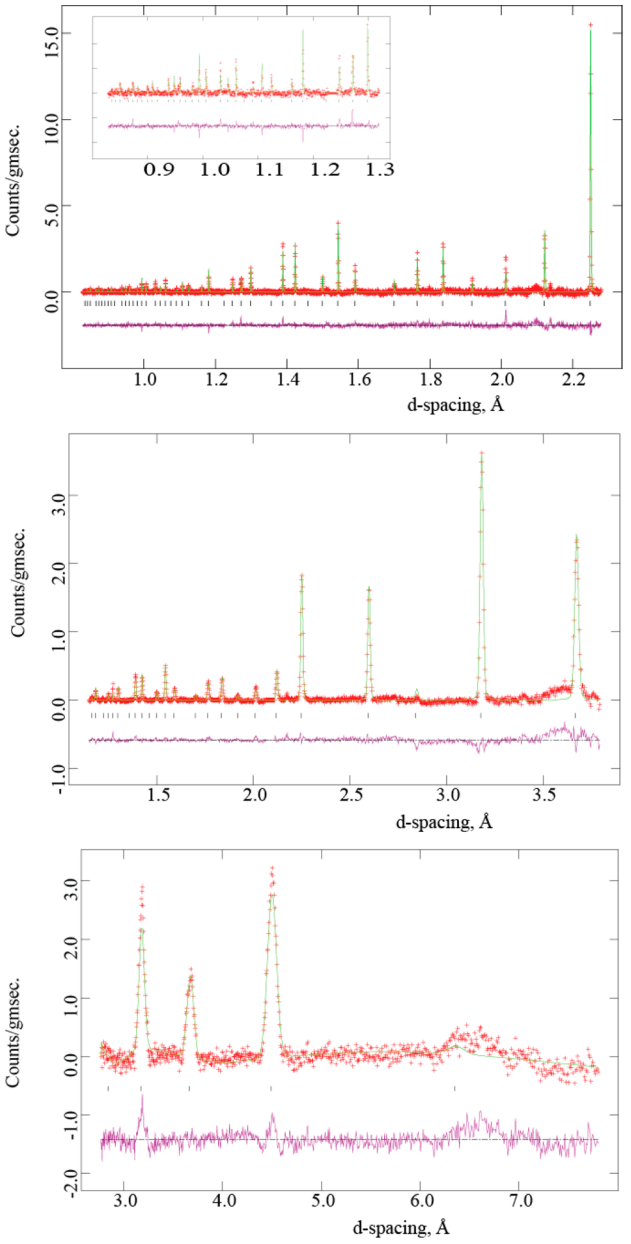

Figure 1. Final profile fits achieved to the neutron powder diffraction data obtained on HRPD from α-FAPI at 298 K. Upper panel, backscattering bank with inset the low d-spacing data magnified; center panel, 90° bank and lower figure the low angle scattering bank. In each profile, crosses represent observed data, upper continuous line the calculated profile, and lower continuous line the difference. Tick marks show calculated reflection positions.

and a statistical analysis of the trajectory are provided in the Supporting Information (Video, Computational section and Figures S6 and S7).

Regarding the low temperature phase behavior, preliminary results indicate that cubic FAPI does undergo a transformation on cooling below room temperature—and by 200 K. Neutron powder data collected at 100 K show a more complex diffraction pattern, which is currently under analysis to determine the unit cell size and any ordering of the FA cation that takes place at low temperatures.

Previous work in the literature describes α-FAPI as being hexagonal,[12] but no evidence of the need to invoke this larger,

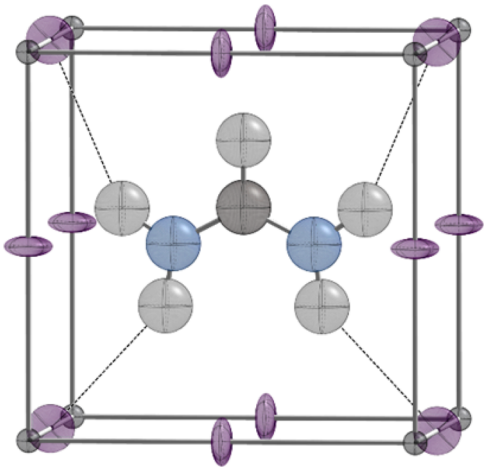

Figure 2. Unit cell structure of α-$[H_2N{-}CH{-}NH_2][PbI_3]$ at 298 K, ADP ellipsoids are shown at 30% probability. Lead (dark gray) at cell corners, iodine (purple) along cell edges, carbon (black), nitrogen (blue), and hydrogen (pale gray). NH···I hydrogen bonds are shown as dotted lines.

more complex unit cell was found in this study, which is much more sensitive to the light atom structural elements. The $[PbI_3]^-$ framework is almost identical in the two studies, with Pb—I bonds near 3.18 Å; PXD patterns generated from the two models are also identical within experimental error. Of note is that faulted and twinned phases at the nanoscale can present themselves as hexagonal to single crystal diffraction methods, such as X-ray and electron diffraction. Recent work on the so-called lonsdaleite phase of diamond found it to consist of solely of cubic phase material that has extensive ⟨113⟩ twins and ⟨111⟩ stacking faults.[21] Given that α-FAPI is normally obtained by a thermally driven phase transition of hexagonal crystals of δ-FAPI it is likely that black FAPI forms as microdomains of twinned or faulted cubic phase material. Indeed our SXD studies of FAPI presented similar unit cells to those reported by Stoumpos but also complex diffraction patterns which could be resolved into multiple cubic twins. It has also been proposed that the conversion of δ-FAPI to α-FAPI might be associated with partial decomposition of the FA cations.[12] Our TGA results from δ-FAPI isolated in this study, Supporting Information Figure S5, show almost no weight loss associated with this process. Indeed, samples of cubic α-FAPI synthesized by the route described in this work (see experimental section) seem relatively stable in comparison with materials described in previous reports. We observe partial, minor conversion back to yellow δ-FAPI after 20 days (see Supporting Information Figure S3).

In conclusion, formamidinium lead iodide adopts a cubic unit cell at room temperature with the FA cations formally disordered over 24 orientations with the perovskitic $[PbI_3]^-$ framework. The molecules are highly rotationally mobile with a turnover frequency of 0.5 THz around room temperature. The structural similarity of the methylammonium and formamidinium lead perovskites has important implications on the understanding, characterization, and stability of their cubic-phase solid-solution, as employed in the current champion efficiency hybrid perovskite solar cells.[10,20]

DOI: 10.1021/acs.jpclett.5b01432
J. Phys. Chem. Lett. 2015, 6, 3209−3212

■ ASSOCIATED CONTENT

Supporting Information

The Supporting Information is available free of charge on the ACS Publications website at DOI: 10.1021/acs.jpclett.5b01432.

Experimental methods (synthesis and data collection), PXD patterns including Le Bail fits, NPD data fitted with hexagonal and cubic unit cells; computational methods (electronic structure and molecular dynamics), and a statistical analysis of the 300 K trajectory. (PDF)

Movie rendering. (MP4)

■ AUTHOR INFORMATION

Corresponding Author

*E-mail: M.T.Weller@bath.ac.uk.

Notes

The authors declare no competing financial interest.

■ ACKNOWLEDGMENTS

O.J.W. would like to thank EPSRC (EP/G03768X/1) for Ph.D. studentship funding via the EPSRC Doctoral Training Centre in Sustainable Chemical Technologies. The experiment at the ISIS Pulsed Neutron and Muon Source was supported by a beamtime allocation from the Science and Technology Facilities Council under Experiment RB1410127. J.M.F. was supported by EPSRC (EP/K016288/1), A.W. was supported by the ERC (Grant No. 277757), and computer time was provided by the U.K.'s HEC Materials Chemistry Consortium, which is funded by EPSRC (EP/L000202).

■ REFERENCES

(1) Snaith, H. J. Perovskites: The Emergence of a New Era for Low-Cost, High-Efficiency Solar Cells. *J. Phys. Chem. Lett.* **2013**, *4*, 3623−3630.

(2) Im, J. H.; Lee, C. R.; Lee, J. W.; Park, S. W.; Park, N. G. 6.5% Efficient Perovskite Quantum-Dot-Sensitized Solar Cell. *Nanoscale* **2011**, *3*, 4088−4093.

(3) Lee, M. M.; Teuscher, J.; Miyasaka, T.; Murakami, T. N.; Snaith, H. J. Efficient Hybrid Solar Cells Based on Meso-Superstructured Organometal Halide Perovskites. *Science* **2012**, *338*, 643−647.

(4) Kim, H. S.; Lee, J. W.; Yantara, N.; Boix, P. P.; Kulkarni, S. A.; Mhaisalkar, S.; Grätzel, M.; Park, N. G. High Efficiency Solid-State Sensitized Solar Cell-Based on Submicrometer Rutile TiO_2 Nanorod and $CH_3NH_3PbI_3$ Perovskite Sensitizer. *Nano Lett.* **2013**, *13*, 2412−2417.

(5) Hu, M.; Liu, L.; Mei, A.; Yang, Y.; Liu, T.; Han, H. Efficient Hole-Conductor-Free, Fully Printable Mesoscopic Perovskite Solar Cells with a Broad Light Harvester $NH_2CH{=}NH_2PbI_3$. *J. Mater. Chem. A* **2014**, *2*, 17115−17121.

(6) Koh, T. M.; Fu, K.; Fang, Y.; Chen, S.; Sum, T. C.; Mathews, N.; Mhaisalkar, S. G.; Boix, P. P.; Baikie, T. Formamidinium-Containing Metal-Halide: An Alternative Material for Near-IR Absorption Perovskite Solar Cells. *J. Phys. Chem. C* **2014**, *118*, 16458−16462.

(7) Lee, J. W.; Seol, D. J.; Cho, A. N.; Park, N. G. High-Efficiency Perovskite Solar Cells Based on the Black Polymorph of $HC(NH_2)_2PbI_3$. *Adv. Mater.* **2014**, *26*, 4991−4998.

(8) Frost, J. M.; Butler, K. T.; Brivio, F.; Hendon, C. H.; van Schilfgaarde, M.; Walsh, A. Atomistic Origins of High-Performance in Hybrid Halide Perovskite Solar Cells. *Nano Lett.* **2014**, *14*, 2584−2590.

(9) Weller, M. T.; Weber, O. J.; Henry, P. F.; Di Pumpo, A. M.; Hansen, T. C. Complete Structure and Cation Orientation in the Perovskite Photovoltaic Methylammonium Lead Iodide between 100 and 352 K. *Chem. Commun.* **2015**, *51*, 4180−4183.

(10) Yang, W. S.; Noh, J. H.; Jeon, N. J.; Kim, Y. C.; Ryu, S.; Seo, J.; Seok, S. I. High-Performance Photovoltaic Perovskite Layers Fabricated through Intramolecular Exchange. *Science* **2015**, *348*, 1234−1237.

(11) Amat, A.; Mosconi, E.; Ronca, E.; Quarti, C.; Umari, P.; Nazeeruddin, M. K.; Grätzel, M.; De Angelis, F. Cation-Induced Band-Gap Tuning in Organohalide Perovskites: Interplay of Spin-Orbit Coupling and Octahedra Tilting. *Nano Lett.* **2014**, *14*, 3608−3616.

(12) Stoumpos, C. C.; Malliakas, C. D.; Kanatzidis, M. G. Semiconducting Tin and Lead Iodide Perovskites with Organic Cations: Phase Transitions, High Mobilities, and near-Infrared Photoluminescent Properties. *Inorg. Chem.* **2013**, *52*, 9019−9038.

(13) Mitzi, D. B.; Liang, K. Synthesis, Resistivity, and Thermal Properties of the Cubic Perovskite $NH_2CH{=}NH_2SnI_3$ and Related Systems. *J. Solid State Chem.* **1997**, *134*, 376−381.

(14) Conings, B.; Drijkoningen, J.; Gauquelin, N.; Babayigit, A.; D'Haen, J.; D'Olieslaeger, L.; Ethirajan, A.; Verbeeck, J.; Manca, J.; Mosconi, E.; et al. Intrinsic Thermal Instability of Methylammonium Lead Trihalide Perovskite. *Adv. Energy Mater.* **2015**, n/a.

(15) Yang, T.; Gregori, G.; Pellet, N.; Grätzel, M.; Maier, J. The Significance of Ion Conduction in a Hybrid Organic−Inorganic Lead-Iodide-Based Perovskite Photosensitizer. *Angew. Chem., Int. Ed.* **2015**, *54*, 7905−7910.

(16) Gottesman, R.; Haltzi, E.; Gouda, L.; Tirosh, S.; Bouhadana, Y.; Zaban, A.; Mosconi, E.; De Angelis, F. Extremely Slow Photoconductivity Response of $CH_3NH_3PbI_3$ Perovskites Suggesting Structural Changes under Working Conditions. *J. Phys. Chem. Lett.* **2014**, *5*, 2662−2669.

(17) Gottesman, R.; Gouda, L.; Kalanoor, B. S.; Haltzi, E.; Tirosh, S.; Rosh-Hodesh, E.; Tischler, Y.; Zaban, A.; Quarti, C.; Mosconi, E.; De Angelis, F. Photoinduced Reversible Structural Transformations in Free-Standing $CH_3NH_3PbI_3$ Perovskite Films. *J. Phys. Chem. Lett.* **2015**, *6*, 2332−2338.

(18) Jeon, N. J.; Noh, J. H.; Yang, W. S.; Kim, Y. C.; Ryu, S.; Seo, J.; Seok, S. Il. Compositional Engineering of Perovskite Materials for High-Performance Solar Cells. *Nature* **2015**, *517*, 476−480.

(19) Eperon, G. E.; Stranks, S. D.; Menelaou, C.; Johnston, M. B.; Herz, L. M.; Snaith, H. J. Formamidinium Lead Trihalide: A Broadly Tunable Perovskite for Efficient Planar Heterojunction Solar Cells. *Energy Environ. Sci.* **2014**, *7*, 982.

(20) Binek, A.; Hanusch, F. C.; Docampo, P.; Bein, T. Stabilization of the Trigonal High Temperature Phase of Formamidinium Lead Iodide. *J. Phys. Chem. Lett.* **2015**, *6*, 1249−1253.

(21) Németh, P.; Garvie, L. A. J.; Aoki, T.; Dubrovinskaia, N.; Dubrovinsky, L.; Buseck, P. R. Lonsdaleite Is Faulted and Twinned Cubic Diamond and Does Not Exist as a Discrete Material. *Nat. Commun.* **2014**, *5*, 5447.

DOI: 10.1021/acs.jpclett.5b01432
J. Phys. Chem. Lett. 2015, 6, 3209−3212